Received: 26 April 2019 | Revised: 6 July 2019 | Accepted: 12 July 2019

DOI: 10.1002/mrm.27930

NOTE

Magnetic Resonance in Medicine

Iterative correction of RF envelope distortion with GRATER-measured waveforms

Vanessa L. Landes[1] | **Krishna S. Nayak**[2]

[1]Department of Biomedical Engineering, Viterbi School of Engineering, University of Southern California, Los Angeles, California

[2]Ming Hsieh Department of Electrical and Computer Engineering, Viterbi School of Engineering, University of Southern California, Los Angeles, California

Correspondence
Vanessa L. Landes, Department of Biomedical Engineering, Viterbi School of Engineering, University of Southern California, 3740 McClintock Ave, EEB 414, Los Angeles, CA 90089-2564.
Email: vlandes@usc.edu

Funding information
National Institutes of Health, Grant/Award Numbers: NIH R01-HL130494.

Purpose: To develop and evaluate a method for RF envelope correction without extra hardware or synchronization.

Methods: Transmitted RF waveforms are measured through a simple pulse sequence called the gradient reversal approach to evaluate RF (GRATER). The measured RF waveforms are used to compute predistorted RF waveforms. This process is repeated until a stopping criterion is met, for example, based on pulse performance or a maximum number of iterations. Excitation profiles and simultaneous multi-slice (SMS) image quality are compared before and after RF predistortion.

Results: The proposed method improved the accuracy of multiband RF pulses, reducing normalized root mean squared error (NRMSE) by >12-fold, and reducing spurious side-lobe excitation by >6-fold. The reduction in unwanted side-lobe signal is demonstrated using SMS bSSFP imaging at 3T in phantoms and in the heart.

Conclusion: Iterative GRATER-based predistortion is a practical, hardware-free way to boost performance of short duration, low flip angle RF pulses, such as those used in SMS bSSFP imaging. Because of its efficiency, this technique could be included as part of an initial scan setup or for use with subsequent scans.

KEYWORDS
iterative correction, RF imperfections, RF pulse design, simultaneous multi-slice imaging

1 | INTRODUCTION

MRI depends on accurate production of RF waveforms for precise excitation. RF pulses with a high peak RF transmit field, and rapid fluctuations in supply current can push the RF subsystem to its limits, leading to RF transmit imperfection.[1,2] This can lead to undesirable effects in several advanced MRI applications, including spurious side-lobe excitation in simultaneous multi-slice imaging.[1,3] A precise excitation profile is especially important for SMS balanced steady-state free precession (bSSFP) imaging. bSSFP imaging necessitates short duration, high flip-angle (FA) RF pulses that are more likely to incur RF transmit imperfection and produce spurious side-lobe excitation. Spuriously excited side lobes are often subject to low FA excitations. If this side lobe is in the stop-band of the bSSFP off-resonance profile, it produces high signal intensity.[4] These extra excited slices can alias into desired slices after reconstruction, producing high signal intensity artifacts with structures from unwanted excited side lobes.

Predistortion techniques have been developed to improve the fidelity of RF excitation by measuring the RF envelope to create new waveforms that correct for expected

Preliminary versions of this work were presented at ISMRM 2018 (Abstract 171), ISMRM 2019 (Abstract 921).

nonlinearity.[1,5-7] These methods require extra hardware, synchronization, and processing to measure transmitted RF waveforms. Recently, the gradient-reversal approach to evaluate RF (GRATER) was introduced as a fast and simple way to measure RF pulses without extra hardware or synchronization.[8] GRATER involves (1) excitation in the presence of a gradient, and (2) immediate signal acquisition in the presence of an inverted gradient along the same axis. GRATER was combined with an outer-volume suppression (OVS) pre-pulse[9] to ensure equal excited signal along the slice-select direction and produce measurements with <2.4% error in a variety of small FA multiband pulses. GRATER, however, had not been used to facilitate predistortion.

In this work, we present a method for iterative correction of RF imperfection with GRATER-measured waveforms. We show that predistorted waveforms can correct for transmission imperfection in a variety of multiband pulses. Finally, we demonstrate improved image quality with predistorted 3-band bSSFP cardiac imaging.

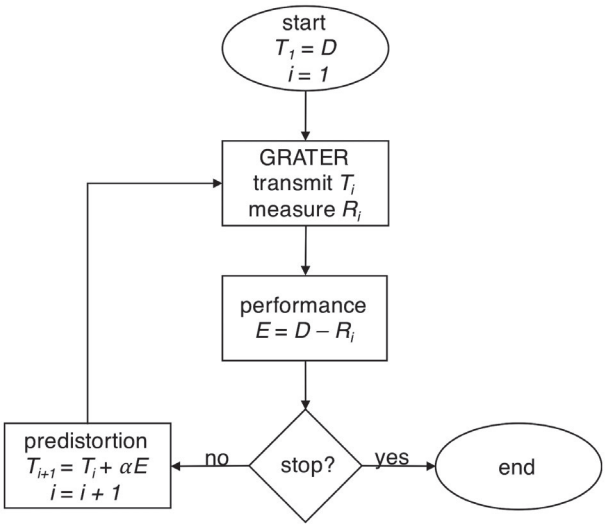

FIGURE 1 The proposed predistortion method consists of a series of GRATER-measurements R_i and creation of predistorted waveforms T_{i+1} until a certain stopping criterion is met, for example, based on a performance threshold and/or a maximum number of iterations. Predistortion consists of (1) determining error E between desired waveform D and R_i, and (2) adding a weighted version of E to the previously transmitted waveform to create a new predistorted waveform

2 | METHODS

Experiments were performed on a clinical 3T MRI Scanner (HD23, GE Healthcare, Waukesha, WI). GRATER measurements were obtained using the body coil and a $60 \times 10 \times 10$ cm cubed rectangular phantom. Final RF waveforms were produced after 40 iterations of GRATER-based predistortion. Forty iterations were used to experimentally demonstrate convergence. SMS bSSFP images were acquired in phantoms and in vivo using an 8-channel cardiac coil.

2.1 | Predistortion technique

RF excitation was improved by correcting for expected errors in transmitted waveforms. Figure 1 illustrates iterative GRATER-based predistortion using a flow-chart. GRATER measurements were performed with the readout gradient amplitude set to half the negative slice-select gradient amplitude; twice the number of RF resolution points were then acquired in the GRATER-measured waveform. This excitation and readout pair took 3.2 ms. The raw measured data was then processed in MATLAB (The MathWorks, Natick, MA) in <2 s, and a new predistorted waveform was created. The next iteration of predistortion would then begin a total of 10 s after the previous measurement. Iteration time was set conservatively at 10 s to ensure complete T_1 relaxation between measurements. GRATER measurement averaging and OVS were not used. The waveform was corrected for off-resonance, T_2^* decay, time-shift, scaling, and initial phase angle calculated during the first iteration. Scaling and time-shift were calculated and updated each iteration. Computation time for an in-house MATLAB implementation was reduced to <2 s (compared to <7 s in Landes and Nayak[8]) by setting the initial guess for initial phase angle as the difference between the mean of the phase angle of the desired waveform and the raw GRATER data.

2.2 | Evaluation: predistortion technique and subsequent RF performance

GRATER-based predistortion was used to measure a variety of multiband pulses with different damping factors α in a uniform rectangular phantom. RF pulses were tested with multi-band (MB) factors MB = 3,4,5 and slice thicknesses to spacing ratios (STR) STR = 2,4. These pulses were designed using the Shinnar-Le Roux algorithm[10] with 648 μs duration, 324 point resolution, FA = 30° (MB = 4,5) or FA = 42° (MB = 3), and optimized phase scheduling.[11] In subsequent experiments, GRATER-based predistortion was performed with $\alpha = 0.25$ to prevent over-shooting the solution.[12]

Experiments performed without and with low-pass filtering of the predistorted waveform to demonstrate impact of filtering to improve data quality and facilitate convergence. The low-pass filter had a cut-off frequency of ±80 kHz. GRATER measurements before predistortion were also examined to determine feasibility of using a scanner-specific distortion function for RF predistortion.

Quality of predistortion was assessed using RMSE between desired and measured waveforms, normalized with

respect to the L2 norm of the desired waveform (NRMSE). Improvement in excitation was evaluated with slice profile measurements, and the mean signal from the largest side lobe was reported. The slice profile was obtained by acquiring multiple GRATER measurements with 15 phase-encodes each along x and y. A 1-s pause was used between measurements to allow for sample relaxation. A total of 648 waveform points were acquired in each GRATER measurement. A long TR was used with phase encoding to ensure sample relaxation between TRs (phantom T_1 was 200 ms). The inverse Fourier transform was then taken, and the signal was discarded except at the center of the phantom. In this way, a frequency profile is obtained along an area with uniform signal.

2.3 | Evaluation: SMS bSSFP imaging

SMS bSSFP images were acquired in phantoms and in vivo. Imaging parameters include TR = 3.2, TE = 1.5, FA = 42°, and per-slice matrix size = 96 × 96. Twelve seconds of dummy acquisitions were performed before imaging to establish steady-state. An MB = 3, STR = 4 pulse was used before and after predistortion to demonstrate differences in image quality. In vivo images were obtained in a healthy volunteer (F, 28) after screening and providing written informed consent with approval from the Institutional Review Board.

A phantom of ABS bricks (LEGO) with a different pattern every 2 cm deep was submerged in water and imaged to indicate aliased signal from extra excited slices. 3-band bSSFP imaging was performed with full-gradient encoding (FGE), center-to-center slice spacing = 20 mm, and slice thickness = 5 mm. Eleven slices were encoded about the 3 excited slices using k_z-gradient encoding.[13] This experiment was performed with and without predistorted waveforms to demonstrate differences in encoded side-lobe signal. The same 3-band experiment was repeated with an added z-shim to create a spatial variation in frequency along the z-axis and illustrate low-flip angle, off-resonant bSSFP imaging (i.e., to demonstrate the need for precise excitation with SMS bSSFP imaging).

This 3-band pulse was again evaluated in vivo and the sequence was adjusted for center-to-center slice spacing = 24 mm and slice thickness = 6 mm. Three short axis slices of the heart were obtained during diastole using (1) single-slice bSSFP imaging, (2) SMS bSSFP imaging with FGE and 3 encoded slices, and (3) SMS bSSFP imaging with blipped-CAIPI encoding (BCE).[13] Single-slice and SMS images with FGE were reconstructed using a simple inverse Fourier transform. SMS images with BCE were reconstructed using split-slice GRAPPA.[14]

3 | RESULTS

The proposed iterative predistortion technique substantially improved RF transmission in all 6 multi-band pulses that were studied. NRMSE between desired and measured waveforms and side-lobe signal were reduced after predistortion (Figure 2A). With low-pass filtering of predistorted waveforms, NRMSE decreased most rapidly over the first 10 iterations and had SD $0.0008 < \sigma < 0.0042$ for subsequent iterations. NRMSE was reduced from <20.1% to <2.7% (Figure 2B). Mean signal from the largest spuriously excited side lobes were <6.6% and <1.1%, before and after predistortion, respectively (Figure 2C). The relative improvement was largest in the MB = 3, STR = 2 pulse with

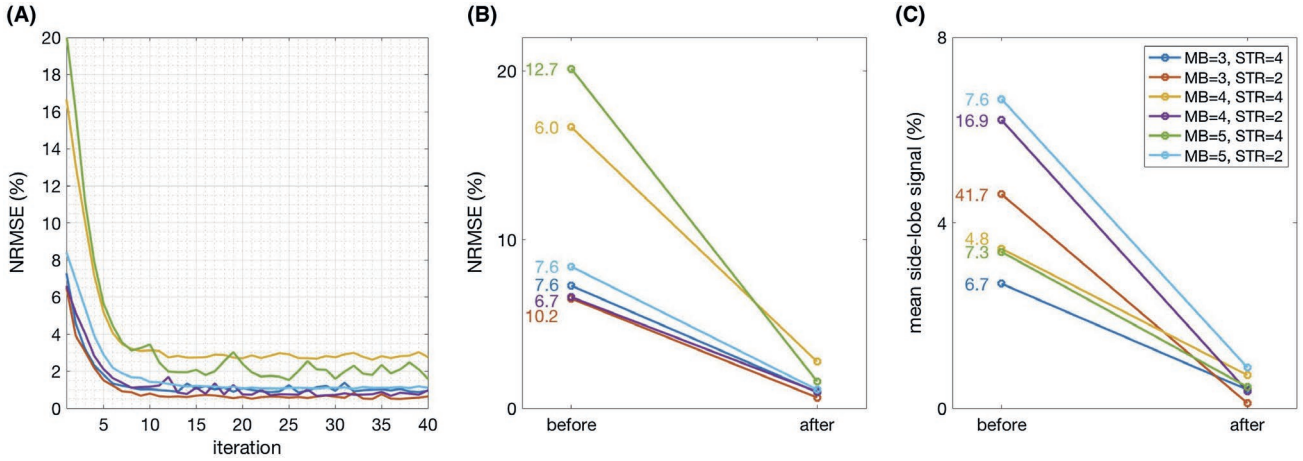

FIGURE 2 Multiband pulses were evaluated in pulses with multi-band (MB) factors of 3, 4, and 5 and slice spacing to thickness ratios (STR) of 4 and 2. (A) NRMSE is shown over 40 iterations of predistortion. NRMSE decreases over the first 10 iterations then remains within 2.7% of its final value. Before and after predistortion, (B) NRMSE was <20.1% and <2.7%, and (C) mean side-lobe signal from the largest side lobe was <6.7% and <1.1%, respectively. Relative improvement (before–after ratio) is listed on the left column for each pulse. Relative improvement ranges from 4.8- to 41.7-fold

41.7-fold reduction in NRMSE and 12.7-fold reduction in mean signal of the largest side lobe. Improvement was lowest in the MB = 4, STR = 4 pulse 4.8-fold reduction in NRMSE, and 6-fold reduction in mean side-lobe signal. For each pulse, the largest spuriously excited side lobe was always next to the main lobe. Without low-pass filtering of the predistorted waveforms, NRMSE diverged after the first 10 iterations in 5 of 6 tested pulses (Supporting Information Figure S1), hence this filtering step was retained for all subsequent experiments. We observed no direct mapping between desired and measured waveforms (Supporting Information Figure S2) that would have allowed a one-step solution.

The slice profile of a MB = 3, STR = 4 pulse matches the desired profile after predistortion (Figure 3). Before predistortion, spurious side-lobe signal has similar spacing and width as the main desired lobes at z = ±4, ±6, ±8, and ±10 cm. Side-lobe intensity is highest closest to the main lobes and decreases with distance from the main lobes. After predistortion, side-lobe signal approaches the noise floor of 0.3% for frequencies below the cutoff frequency of the predistorted waveform's low-pass filter. Side-lobe signal before predistortion is <0.7% for frequencies above this cutoff frequency and is not significantly reduced after predistortion.

Reduction in side-lobe excitation is seen after predistortion in a LEGO phantom with 3-band bSSFP imaging, FGE, and 12 encoded slices (Figure 4). Before predistortion, encoded image signal about z = −4 cm was highest with mean/max = 6.7%/0.74% compared to the reference image, respectively. After predistortion, encoded signal approached the level of noise; this is apparent in both the measured z-profile and the encoded image. In other words, no spurious side-lobe signal was measured or encoded, indicating an improvement in RF excitation. Signal in the slice at z = 4 cm contains features from the desired reference slice at z = −2 cm, likely because of imperfections in 3D encoding.

Off-resonant side-lobe excitation was also reduced after predistortion (Supporting Information Figure S3). The

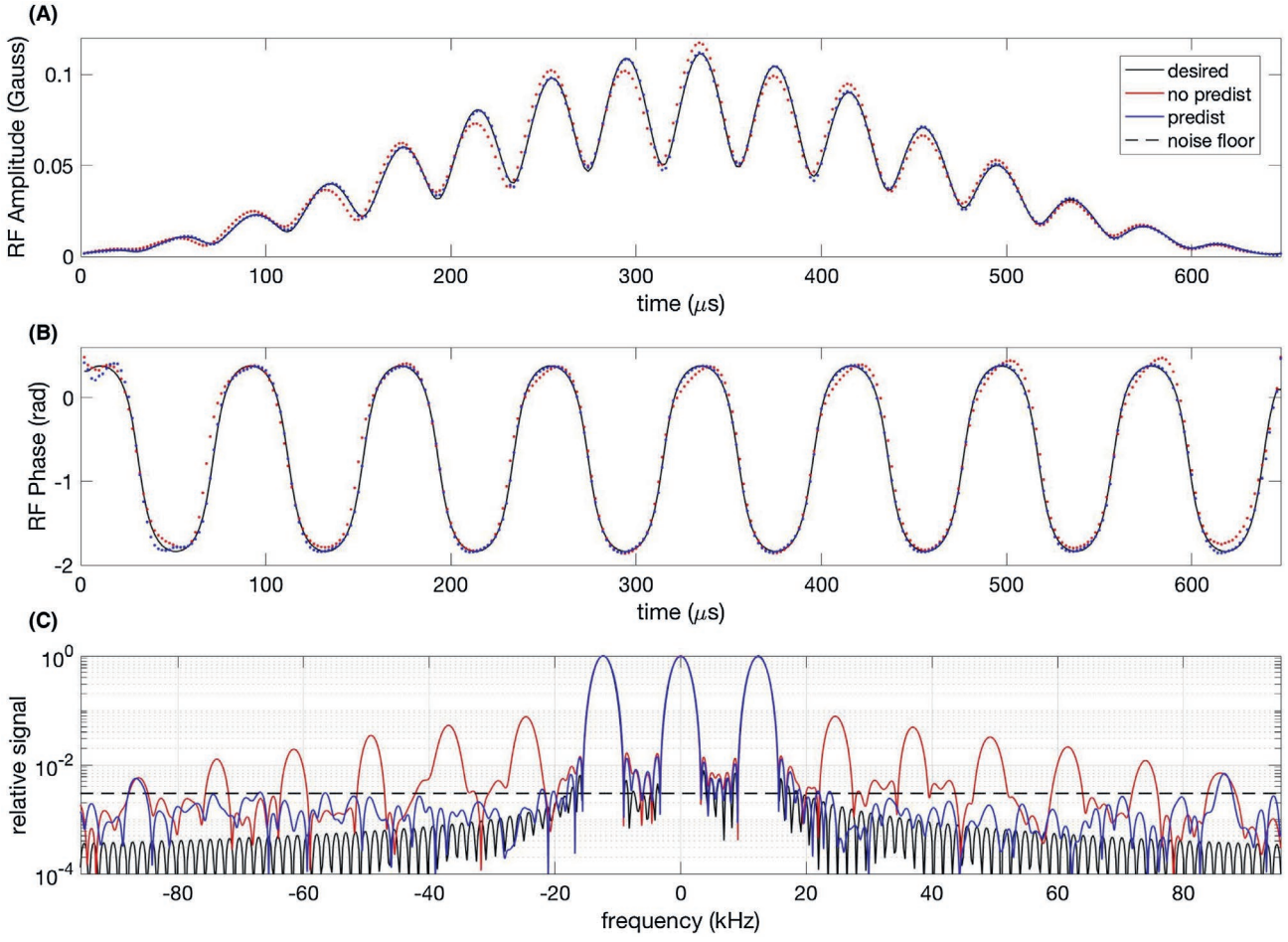

FIGURE 3 Amplitude and phase components of MB = 3 and STR = 4 waveforms (A and B) are shown with their corresponding excitation profiles (C) using (1) Bloch simulations and the desired waveform, (2) experimental measurements and the waveform before predistortion, and (3) experimental measurements and the waveform after predistortion. Excitation profiles are on a log scale to accentuate side-lobe behavior. NRMSE between desired and measured waveforms is reduced from 7.4% to 0.9% with predistortion. Spurious side lobes are reduced from <7.6% to <0.32% for frequencies between ±80 kHz (the low-pass filter cutoff frequency). This approaches the noise floor of 0.3%

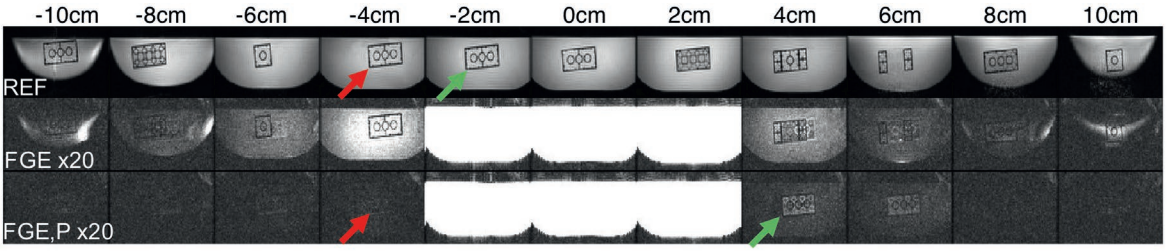

FIGURE 4 Phantom with 3-band bSSFP imaging, full-gradient encoding (FGE), and 11 encoded slices (z = −10:2:10 cm) is shown next to single-band reference slices (row 1) before (row 2) and after (row 3) predistortion. Without windowing, 3 excited slices are comparable to the reference slices (±2 and 0 cm), and there is no visually detectable signal in the extra encoded slices. With windowing, extra excited side lobes are seen with features from reference slices (red arrows). After predistortion, extra encoded signal is reduced. Signal in the slice at z = 4 cm contains features from the desired slice at 2 cm (green arrows)

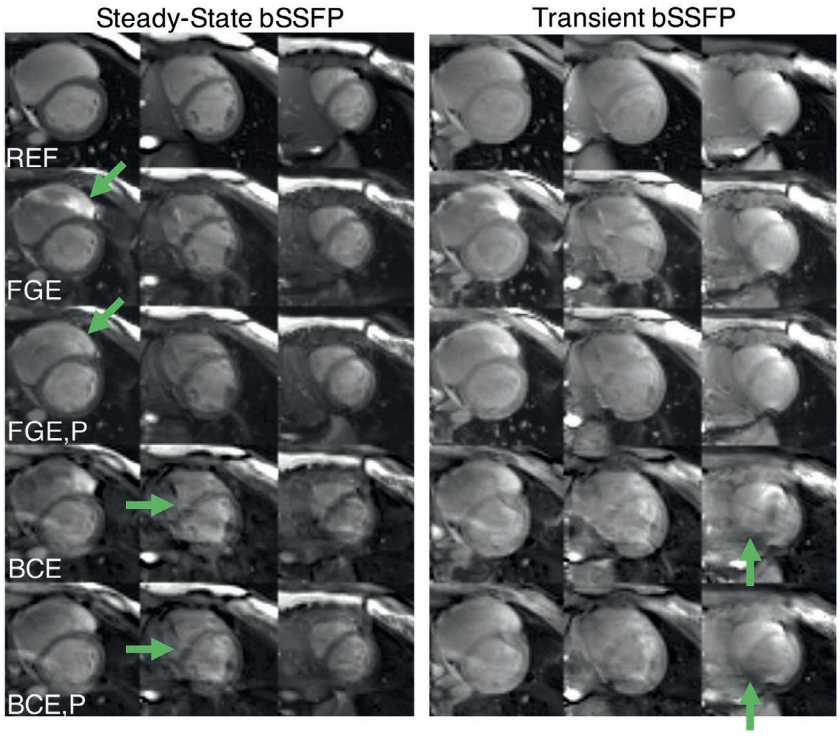

FIGURE 5 Steady-state (left) and transient (right) bSSFP images of the basal, mid, and apical short-axis slices of the heart. Single-slice reference (REF) images are shown next to SMS images with full-gradient encoding (FGE) and blipped-CAIPI encoding (BCE) before and after predistortion (P). Artifacts because of RF transmit error are reduced after predistortion in each SMS image with both FGE and BCE (green arrows). Additional artifacts are still present in SMS images with BCE, because of the aggressive acceleration (R = 3) with low channel count (8-channel cardiac array)

intensity of excited off-resonant signal was highest before predistortion in slices at z = 4 cm (mean/max signal: 33.5%/103.0% of main lobes). After predistortion, encoded signal was reduced to mean/max signal: 4.2%/10.98%. After predistortion, residual signal contained features from the desired slices about z = −2 cm as well as the side lobe at z = 4 cm.

SMS bSSFP artifacts were reduced after predistortion in vivo with FGE and BCE (Figure 5); features in (left to right) basal, mid, and apical short axes slices are discernable after predistortion. Image quality between reference and SMS bSSFP images with FGE are comparable after predistortion. Image quality is improved in SMS bSSFP imaging with BCE after predistortion. Additional artifacts are still present, because of the aggressive acceleration (R = 3) with low channel count (8-channel cardiac array).[15]

4 | DISCUSSION

Iterative GRATER-based predistortion improved multiband pulse performance with >12-fold reduction in NRMSE and >6-fold reduction in max side-lobe signal. Predistorted waveforms were used with SMS bSSFP imaging to successfully reduce excitation artifacts. This technique could be especially beneficial for in vivo SMS bSSFP cardiac imaging. Cardiac muscle has a low T_2–T_1 ratio compared to fat and a low relative signal intensity. When off-resonant fat is excited in a spuriously excited side lobe, it can alias into the myocardium, confounding image quality. This low-flip angle, off-resonant, high-signal excitation was demonstrated with the added z-shim in lego phantom images and in vivo cardiac images. This technique could also be useful in situations where precise excitation is desirable, including other SMS

imaging applications, MR spectroscopy,[16] and hyperpolarized lung imaging.[17]

The main advantage of using GRATER-based predistortion is that it does not require any extra hardware to measure RF envelopes. However, GRATER comes with several disadvantages, including potential biases because of object non-uniformity, nonlinearity of the excited signal with higher flip angles, and sensitivity to noise.[8] Despite these disadvantages, these experiments demonstrated significant improvement in RF excitation after predistortion and <2.7% NRMSE. Remaining NRMSE could stem from inaccuracies in GRATER measurements. The GRATER technique assumes each excited slice contributes equal signal. It is possible error was introduced into the measurements because of unintended RF excitation outside the phantom's volume of $60 \times 10 \times 10$ cm^3. If this is the case, NRMSE can be reduced by increasing the size of the phantom used for predistortion. It is also possible that off-resonance introduced error in GRATER measurements. In this situation, averaging measurements and an OVS pre-pulse could reduce error.

Iterative RF predistortion using a pulse-sequence-based RF measurement technique has been previously demonstrated.[18] There are 2 differences between the Lebsack and Wright[18] work and our work. First, the previous RF measurement technique uses a spin-echo (SE) pulse, whereas GRATER does not. SE introduces some risk of scaling error because of imperfections in the SE pulse. In addition, SE cannot be used with a short TR, and GRATER measurements are substantially faster (10 ms). Second, the previous iteration scheme compares desired and measured magnetization profiles. A windowed version of the Fourier transform of the difference between profiles was taken and scaled by a damping factor to produce updated RF waveforms. The damping factor changed during each iteration based on differences between magnetization profiles. This ensured stability of technique. GRATER-based predistortion uses measured and desired RF waveforms directly, does not dynamically update the damping factor, and stability has been demonstrated in this work.

Forty iterations were sufficient to demonstrate feasibility of GRATER-based predistortion. NRMSE did not increase after 10 iterations if a low-pass filter was applied to the predistorted waveform. With 10 s per iteration, predistortion of each waveform took almost 7 min, which is needlessly long and not practical for the clinical setting. We expect that 10 iterations with a repetition time on the order of 2 s is more than adequate and will be practical clinically. This time can be further shortened using a more sophisticated iteration and stopping criterion. In these experiments, for example, choosing a stopping criterion as ΔNRMSE <0.1% between iterations would have allowed for a solution to be reached within 10 iterations. Other stopping criterion could be to stop iterative predistortion when a certain NRMSE or spurious side-lobe signal level has been reached.

The chosen update direction was simply the difference between desired and measured waveforms in an effort to minimize NRMSE between these waveforms.[19] If an approximated derivative were available for this NRMSE function being minimized, other more sophisticated schemes could be used, such as gradient descent. Unfortunately, no clear relationship was discernable between the distortion in measured RF pulses and desired pulses in this study. Estimating the gradients is a topic for future research. The current method works with few iterations, is fast, and is easy to implement. A gradient-based likely would not accelerate convergence compared to the current implementation but could potentially achieve lower NRMSE.

A limitation of this study is that GRATER-based predistortion was not compared with an alternative technique such as the pick-up coil approach.[1] RF measurements made with GRATER and the pick-up coil method proved comparable,[8] however, equivalence in the context of pre-distortion remains future work.

5 | CONCLUSION

This study demonstrates feasibility of iterative GRATER-based RF predistortion as part of an initial sequence setup to improve image quality in later scans. This could be useful for a wide range of RF pulses with high peak B_1^+ and rapid current oscillations that could incur nonlinearity, or with low-cost RF amplifiers with a limited linearity range. This technique is likely to be critical for SMS bSSFP imaging at 3T where short, high flip angle RF pulses are desirable but also likely to produce side-lobe excitation that can alias back into the desired slices.

ACKNOWLEDGMENTS

We thank NIH (R01-HL130494) for support.

ORCID

Vanessa L. Landes http://orcid.org/0000-0001-6610-7335

REFERENCES

1. Zhu K, Dougherty RF, Middione MJ, et al. RF Amplifier nonlinearity correction for multiband RF pulses. In Proceedings of the 23rd Annual Meeting of ISMRM, Toronto, Canada, 2015. p. 1830.
2. Razavi B. Basic concepts in RF design. In: Rappaport T, ed. *RF Microelectronics*. Upper Saddle River: Prentice-Hall; 2013:11–22.

3. Chan F, Pauly J, Macovski A. Effects of RF amplifier distortion on selective excitation and their correction by prewarping. *Magn Reson Med*. 1992;23:224–238.
4. Hargreaves B. Bloch simulation equation. http://mrsrl.stanford.edu/~brian/bloch/. Updated July 5, 2002. Accessed April 15, 2017.
5. Stang P, Kerr AB, Grissom W, Pauly JM, Scott GC. Vector iterative pre-distortion: an auto-calibration method for transmit arrays. In Proceedings of the 17th Annual Meeting of ISMRM, Honolulu, HI, 2009. p. 395.
6. Zanchi MG, Stang P, Kerr A, Pauly JM, Scott GC. Frequency-offset cartesian feedback for MRI power amplifier linearization. *IEEE Trans Med Imaging*. 2011;30:512–522.
7. Hoult DI, Kolansky G, Kripiakevich D, King SB. The NMR multi-transmit phased array: a Cartesian feedback approach. *J Magn Reson*. 2004;171:64–70.
8. Landes VL, Nayak KS. Simple method for RF pulse measurement using gradient reversal. *Magn Reson Med*. 2018;79:2642–2651.
9. Smith TB, Nayak KS. Reduced field of view MRI with rapid, B 1-robust outer volume suppression. *Magn Reson Med*. 2012;67:1316–1323.
10. Cunningham CH, Wood ML. Method for Improved multiband excitation profiles using the Shinnar-Le Roux Ttransform. *Magn Reson Med*. 1999;42:577–584.
11. Wong E. Optimized phase schedules for minimizing peak RF power in simultaneous multi-slice RF excitation pulses. In Proceedings of the 20th Annual Meeting of ISMRM, Melbourne, Australia, 2012. p. 2209.
12. Landes V, Nayak KS. Improved multi-band RF performance using GRATER-based predistort. In Proceedings of the 26th Annual Meeting of ISMRM, Paris, France, 2018. p. 171.
13. Setsompop K, Gagoski BA, Polimeni JR, Witzel T, Wedeen VJ, Wald LL. Blipped-controlled aliasing in parallel imaging for simultaneous multislice echo planar imaging with reduced g-factor penalty. *Magn Reson Med*. 2012;67:1210–1224.
14. Cauley SF, Polimeni JR, Bhat H, Wald LL, Setsompop K. Interslice leakage artifact reduction technique for simultaneous multislice acquisitions. *Magn Reson Med*. 2014;72:93–102.
15. Reeder SB, Wintersperger BJ, Dietrich O, et al. Practical approaches to the evaluation of signal-to-noise ratio performance with parallel imaging: application with cardiac imaging and a 32-channel cardiac coil. *Magn Reson Med*. 2005;54:748–754.
16. Kreis R. Issues of spectral quality in clinical 1H-magnetic resonance spectroscopy and a gallery of artifacts. *NMR Biomed*. 2004;17:361–381.
17. Kaushik SS, Freeman MS, Cleveland ZI, et al. Probing the regional distribution of pulmonary gas exchange through single-breath gas- and dissolved-phase 129Xe MR imaging. *J Appl Physiol*. 2013;115:850–860.
18. Lebsack ET, Wright SM. Iterative RF pulse refinement for magnetic resonance imaging. *IEEE Trans Biomed Eng*. 2002;49:41–48.
19. Scherzer O. Convergence criteria of iterative methods based on landweber iteration for solving nonlinear problems. *J Math Anal Appl*. 1995;194:911–933.
20. Vannesjo SJ, Haeberlin M, Kasper L, et al. Gradient system characterization by impulse response measurements with a dynamic field camera. *Magn Reson Med*. 2013;69:583–593.

SUPPORTING INFORMATION

Additional supporting information may be found online in the Supporting Information section at the end of the article.

FIGURE S1 NRMSE between desired and measured waveforms for 1 to 40 iterations of predistortion, (A) with low-pass filtering of the predistorted waveform, and (B) without low-pass filtering. Without low-pass filtering, NRMSE steadily increases after iteration 10 in each example except for in the MB = 3, STR = 4 pulse

FIGURE S2 The real, imaginary, amplitude, and phase components of desired and measured waveforms before predistortion. We observed no direct mapping between desired and measured RF waveforms. Estimating the gradient is a topic for future research (this has been demonstrated successfully with gradient nonlinearity corrections).[20] Instead, this article proposes a pulse-specific method to improve RF performance

FIGURE S3 Phantom with 3-band bSSFP imaging, full-gradient encoding (FGE), 11 encoded slices, and added off-resonance is shown next to single-band reference slices (row 1) before (rows 2–3) and after (rows 4–5) predistortion. Before predistortion, main lobe signal has different signal intensity compared to the reference slices and off-resonant side-lobe excitation has higher signal variation than on-resonant (see Figure 5). Side-lobe signal is reduced after predistortion (red arrows) and residual encoded signal contains features from the desired slices (green arrows)

How to cite this article: Landes VL, Nayak KS. Iterative correction of RF envelope distortion with GRATER-measured waveforms. *Magn Reson Med*. 2020;83:188–194. https://doi.org/10.1002/mrm.27930